

The British University in Egypt

BUE Scholar

Pharmacy

Health Sciences

Winter 12-15-2022

Karafsin, a Unique Mono-acylated Flavonoid Apiofurnoside from the Leaves of *Apium graveolens* var. *secalinum* Alef: In vitro and In vivo Anti-inflammatory Assessment

Noha Swilam

The British University in Egypt, noha.swilam@bue.edu.eg

Mahmoud Nawwar

National Research Centre, Department of Phytochemistry and Plant Systematic

Eman Mostafa

Faculty of Pharmacy, October University of Modern Sciences and Arts (MSA University)

Dalia Mostafa

Faculty of Pharmacy, October University of Modern Sciences and Arts (MSA University)

Mai Ragab

Faculty of Pharmacy, October University of Modern Sciences and Arts (MSA University)

Follow this and additional works at: <https://buescholar.bue.edu.eg/pharmacy>



Part of the [Natural Products Chemistry and Pharmacognosy Commons](#)

Recommended Citation

Swilam, Noha; Nawwar, Mahmoud; Mostafa, Eman; Mostafa, Dalia; and Ragab, Mai, "Karafsin, a Unique Mono-acylated Flavonoid Apiofurnoside from the Leaves of *Apium graveolens* var. *secalinum* Alef: In vitro and In vivo Anti-inflammatory Assessment" (2022). *Pharmacy*. 663.

<https://buescholar.bue.edu.eg/pharmacy/663>

This Article is brought to you for free and open access by the Health Sciences at BUE Scholar. It has been accepted for inclusion in Pharmacy by an authorized administrator of BUE Scholar. For more information, please contact bue.scholar@gmail.com.



Karafsin, a unique mono-acylated flavonoid apiofurnoside from the leaves of *Apium graveolens* var. *secalinum* Alef: *In vitro* and *in vivo* anti-inflammatory assessment

Eman S. Mostafa^a, Mahmoud A.M. Nawwar^b, Dalia A. Mostafa^c, Mai F. Ragab^d, Noha Swilam^{e,*}

^a Department of Pharmacognosy, Faculty of Pharmacy, October University of Modern Sciences and Arts (MSA University), Giza, Egypt

^b National Research Centre, Department of Phytochemistry and Plant Systematic, Dokki, Cairo, Egypt

^c Department of Pharmaceutics, Faculty of Pharmacy, October University of Modern Sciences and Arts (MSA University), Giza, Egypt

^d Department of Pharmacology and Toxicology, Faculty of Pharmacy, October University of Modern Sciences and Arts (MSA University), Giza, Egypt

^e Department of Pharmacognosy, Faculty of Pharmacy, The British University in Egypt (BUE), Egypt

ARTICLE INFO

Keywords:

Apium graveolens var. *secalinum* Alef
Apigenin 7-*O*-mono-apiofuranoside
apigenin-7-*O*-β-(5'-*E*-*p*-coumaroyl)-
apiofuranoside
Antioxidant
Anti-inflammatory
Rat paw edema

ABSTRACT

Celery ethanol extract (CEE) of leaves of *Apium graveolens* var. *secalinum* Alef, showed high phenolic content with significant antioxidant activity using DPPH and ORAC assay. Two unique unknown compounds, apigenin 7-*O*-mono-apiofuranoside and acylated flavonoid, 7-*O*- (5'-*E*-*p*-coumaroyl)-apiofuranoside (karafsin) were identified in CEE for the first time by a full structural analysis, along with 6 known compounds. While karafsin significantly inhibited cyclooxygenase-2 by 42.52 ± 2.88 and 70.33 ± 2.97 % at 50 and 100 mg/mL and 5-lipoxygenase by 37.33 ± 2.87 and 75.77 ± 2.57 % at 50 and 100 mg/mL in raw macrophage cells challenged with *Escherichia coli* lipopolysaccharide, CEE exhibited the same weigh-dose activity as a crude extract mixture. Comparable inhibition of NO was also observed by CEE versus karafsin at approximately 0.06 mg/mL. Thus, CEE as a mixture has potent anti-inflammatory activity, of which the formulated 1% topical gel was found to have a 79.51 % inhibition of edema in the carrageenan-induced rat paw model, comparable as the commercial 1% diclofenac gel. CEE has potent anti-inflammatory activity and this warrants additional investigations.

1. Introduction

Inflammation is a series of complex changes that occurs in living tissues in response to damage or injury and usually accompanied by ache and pain. It is a central feature of many pathophysiological conditions such as cardiovascular diseases, metabolic syndromes, diabetes, obesity and even several cancer types (Moro et al., 2012). When cells are exposed to immune stimulants, the pro-inflammatory cells, such as macrophages, monocytes, or other host cells, start to produce cytokines and other mediators, which initiate the inflammation process that embraces increased vascular permeability, protein denaturation and alterations to the cell membrane. This could be a lead to the activation of several enzymes such as cyclooxygenase-2 (COX-2) and 5-lipoxygenase (5-LOX) which metabolize arachidonic acid and consequently production of inflammatory mediators, such as prostaglandin E2 (PGE2) and

leukotrienes, respectively. Besides, in hypoxic conditions, nitric oxide (NO) which is one of the inflammatory mediators, produced by the activation of inducible nitric oxide synthase (iNOS) (Poyton et al., 2009). Overproduction of these inflammatory mediators leads to different kinds of cell damage. In fact, inhibition of these enzymes result in reduced production of prostaglandins and leukotrienes. A drug that inhibit these enzymes is considered to have the ability to provide analgesic and anti-inflammatory effects with reduction in gastro-intestinal side-effects (Langhansova et al., 2017). Moreover, the inflammation mechanisms also involve reactive oxygen species (ROS). ROS are mainly triggered as a result of oxidative stress and is started by the activation of leukotrienes. Many chronic diseases are caused by the inflammation associated with oxidative stress. Cellular respiration by mitochondrial oxidative metabolism in the cell results in the production of peroxides and ROS (Liemburg-Apers et al., 2015). Also, in hypoxic conditions,

* Corresponding author at: Department of Pharmacognosy, Faculty of Pharmacy, The British University in Egypt, El Sherouk City, Suez Desert Road, Cairo, 11837, P.O. Box 43, Egypt.

E-mail address: noha.swilam@bue.edu.eg (N. Swilam).

<https://doi.org/10.1016/j.indcrop.2020.112901>

Received 5 June 2020; Received in revised form 21 August 2020; Accepted 25 August 2020

Available online 3 October 2020

0926-6690/© 2020 Elsevier B.V. All rights reserved.

nitric oxide (NO) is produced during respiratory chain reaction. This latter reactive nitrogen species (RNS) may further lead to the production of reactive species like reactive malondialdehyde, 4-hydroxynonenal and aldehydes. Indeed, increased production of ROS/RNS may result in irreversible cellular damage that can lead to the cell death. Nowadays, anti-inflammatory drugs cause many side effects (Ramana et al., 2014). For example, non-steroidal anti-inflammatory drugs (NSAIDs) causes gastrointestinal disorders conditions. In addition, they can increase the risk of renal impairment, myocardial infarction and stroke (Al-Saeed, 2011). In view of this facts, many natural products have shown a safety profile and gained wide acceptance nowadays (Hörl, 2010) and become of a particular interest as a lead for bioactive molecules for the management, treatment and control of several inflammatory mediated diseases (Abdou et al., 2013; Akanda et al., 2019). Polyphenols (such as flavonoids and phenolic acids) have been reported to be useful as adjuvant therapy for their potential anti-inflammatory effect, associated with their antioxidant activities and inhibition of enzymes involved in the inflammatory pathways (Hussain et al., 2016). Therefore, screening of the antioxidant activities may provide important information about the potential anti-inflammatory activity of a certain drug.

Apium graveolens L., celery, is a plant belonging to the family Apiaceae and includes three varieties, namely, *Apium graveolens* var. dulce, *Apium graveolens* var. rapaceum, and *A. graveolens* var. secalinum Alef. *Apium graveolens* var. secalinum Alef is the most popular variety of celery in Asian countries and Mediterranean region (Rubatzky and Yamaguchi, 1997). The plant is known in English as leaf or chinese celery and in Egypt as Karafs. The stems of this variety are thinner than those of the other two celery varieties (Western celery) and its stalks take round, hollow shapes. Also, unlike with Western celery, the leaves and the stalks of this variety are used for its edible and flavorful properties (Larkcom, 2008). Among the different biological activities of celery, an extract from *A. graveolens* var. secalinum is used as neuroprotective in brain diseases (Malhotra, 2006; Zhang et al., 2018). Among the three celery varieties, it is recognized that the most extended variety, *A. graveolens* var. secalinum Alef has not been subjected to extensive phytochemical study for the phenolics of its leaves, though the essential oil of the seeds of the plant have been fully investigated (Kooti and Daraei, 2017). During current continuing search for novel bioactive metabolites from Egyptian plants, the aqueous ethanol extract of the leaves of, *A. graveolens* var. secalinum Alef, was selected to be the subject of thorough investigation in the present work. CEE of the leaves revealed, in its two dimensional paper chromatograms (TDPC) a recognizable phenolic profile. The present study reports on the isolation and structure determination of polyphenols from CEE. In addition, in view of the recorded antioxidant activity for CEE and isolate by DPPH and ORAC assay, *in-vitro* assessment for anti-inflammatory activity was accomplished. Besides, *in-vivo* anti-inflammatory activity for the CEE using method of carrageenan-induced rat paw edema was also, assayed.

2. Material and methods

2.1. General

NMR spectra were developed in DMSO- d_6 in a Bruker 400 MHz NMR spectrometer, at 400 MHz. Standard pulse sequence and parameters were used to obtain one-dimensional ^1H and ^{13}C spectra. ^1H chemical shifts (δ) were measured in ppm, relative to TMS and ^{13}C NMR chemical shifts to DMSO- d_6 and were converted to TMS scale by adding 39.5. ^1H - ^{13}C heteronuclear single quantum coherence (HSQC), and heteronuclear multiple bond coherence (HMBC) were obtained by employing the conventional pulse sequences. High resolution ESI mass spectra were measured using a Finnigan LTQ FT Ultra mass spectrometer (Thermo Fisher Scientific, Bremen, Germany) equipped with a Nanomate ESI interface (Advion Biosystems, USA). An electrospray voltage of 1.7 kV (+/-) and a transfer capillary temperature of 200 °C were applied. High resolution product ions were detected in the Fourier

transform ion cyclotron resonance (FTICR) cell of the mass spectrometer. UV recording was made on a Shimadzu UV-vis-1601 spectrophotometer. Paper chromatographic analysis (PC) was carried out on Whatman No. 1 paper, using solvent systems: (1) H₂O; (2) 2% HOAc (acetic acid: H₂O, 98:2); (3) BAW (*n*-BuOH-HOAc-H₂O, 4:1:5, upper layer); (4) B BPW (Benzene-*n*-BuOH-Pyridine- H₂O, 1:5:3:3, upper layer), all solvents are of HPLC grades (Sigma-Aldrich, US).

2.2. Plant materials

Collection of leaf celery, Karafs was made at a farm in Nile Delta, 35 Km north of Cairo, in June 2019. Authentication was achieved by Dr. S. Kawashty, Prof of Botany, National Research Centre (NRC), Giza, Egypt. Voucher specimen (K, 32) was deposited at the herbarium of the NRC.

2.3. Preparation of extract

Fresh leaves of celery (2 kg), was homogenized in EtO-H₂O (3:1) (three extractions each with (2000 mL). The filtrate was then dried under reduced pressure at 50 °C to yield dark brown amorphous material (100 g).

2.4. Estimation of the total phenolic and flavonoid contents

The total phenolic content was calculated as gallic acid equivalents (GAE) per g of sample using Folin-Ciocalteu reagent and a calibration curve prepared with gallic acid. Moreover, the total flavonoid content was determined as catechin equivalents (CE) per g of sample using an aluminium chloride (AlCl₃) colorimetric assay (Zilic et al., 2012).

2.4.1. Isolation of polyphenols 1–8

CEE was found to contain a complicated mixture of phenolics, which includes mainly phenyl propanoids as detected by 2-dimensional paper chromatographic screening (TDPC, spots of fluorescent blue, or greenish blue color, under UV light). The chromatograms revealed in addition the presence of two dark purple spots which turned lemon yellow when fumed with ammonia vapor, thus suggesting its flavonoid nature. The search for new, potentially biologically active compounds becomes much more efficient after sorting out all the known structures in that mixture through exhaustive extraction of the parent extract (70 g) under reflux by ethyl acetate for eight h and the subsequent analysis by TDPC.

2.4.2. Isolation of the new compounds 1 and 2

The residue left after ethyl acetate extraction (67.9 g) was shown by TDPC to contain mainly the two previously detected flavonoids appearing on the chromatograms as two distinct dark purple spots under UV light. A portion (62.5 g) of that residue was then applied to a Sephadex LH-20 (450 g) column (100 × 5 cm) and eluted with H₂O followed by H₂O/MeOH mixtures of decreasing polarities. The elution process was monitoring the column under UV light whereby, two dark purple bands migrated successively along the column. They are individually desorbed by 30 and 50 % aqueous MeOH to yield 180 mg of crude compound 1 eluted by 30 % and 400 mg of crude compound 2 eluted by 50 % aqueous methanol (TDPC). Purification of the crude materials thus received after removing of the solvent, was achieved by applying each, individually to an MCI gel column eluted by *n*-butanol water saturated. Repeating the MCI gel column process twice led to the desorption of chromatographically pure samples of 1 (39 mg) and of 2 (130 mg), respectively.

2.4.3. Isolation of known compounds 3–8

Compounds 3–8 were individually separated from the ethyl acetate extract by repeated preparative paper chromatography (prep. PC) using Whatmann paper number 3 MM and H₂O: acetic acid (94:6) mixture as solvent. Repeated Prep.PC, twice afforded pure chromatographic

samples of each of known compounds 3–8.

2.4.4. Apigenin-7-O- β -apiofuranoside 1

Faint brown amorphous powder, R_f -values: 0.33 (H₂O), 0.48 (HOAc), 0.35 (BAW). UV λ_{\max} nm in MeOH: 268, 330; NaOAc: 268, 332; NaOC-H₃BO₃: 267, 380; AlCl₃: 276, 297, 380; NaOMe: 270, 299, 378. HRFIMS: (negative mode): [M-H]⁻ ion at m/z = 401.3431 (calcd. for C₂₀H₁₇O₉, m/z = 401.344355 Da). Normal acid hydrolysis by 2 N aqueous HCl, for two h gave: abiofuranoseo (CoPC): (R_f values X 100), Solvent (3): β -apiofuranose = 20; sugar markers: arabinose = 26.28, xylose = 30.28, rhamnose = 40.0; solvent (4): β -apiofuranose = 23; sugar markers: arabinose = 27.9, xylose = 33, rhamnose = 42, and apigenin: R_f -values [0.88 (BAW), 0.15 6% AcOH, 0.05 (H₂O)], UV λ_{\max} in MeOH: 269, 330. NMR data of 1: Apigenin moiety: ppm δ 7.97 (2H, d, J = 8 Hz, H-2', H-6'); 6.95 (2H, d, J = 8 Hz, H-3', H-5'), 6.42 (1 H, d, J = 2.5 Hz, H-6); δ 6.85 (1 H, d, J = 2.5 Hz, H-8); 6.88 (1 H, singlet, H-3); apiofuranoside moiety: ppm 5.40 (1H, broad singlet, half line width, $\Delta\nu_{1/2}$ = 4 Hz, anomeric proton), four resonances between δ 4.30 and δ 3.20 interfered by water protons and apigenin phenolic proton resonances. ¹³C NMR data of apigenin-7-O- β -apiofuranoside (Table 1).

2.4.5. Apigenin-7-O- β -(5''-E-p-coumaroyl)- β -apiofuranoside, Karafsin 2

Light brown amorphous powder, R_f -values: 0.38 (H₂O), 0.52 (HOAc), 0.41 (BAW). UV λ_{\max} nm in MeOH: 269, 330; NaOAc: 256.0, 268, 339.8; NaOC-H₃BO₃: 258.0, 267, 348.6; AlCl₃: 276, 298, 345.2; NaOMe: 265.0, 389.8. HRFIMS: [M-H]⁻ 547.4889 corresponding to a molecular weight (Mr) 548 D, molecular formula of C₂₉H₂₃O₁₁ (calcd 547.4876); ESI-MS-MS: m/z 401 [M-H-146]- and m/z 269 [M-H-146-132]- Normal acid hydrolysis (2 N aqueous HCl, 2 h) gave apiofuranoseo (R_f values X 100): Solvent (3) 20, solvent (4) 23; *p*-coumaric acid: R_f values: 0.88 BAW, 0.15 6% AcOH, 0.05 H₂O; UV λ_{\max} in MeOH: 269, 330; and apigenin. ¹H NMR data of 2: apigenin moiety: ppm δ 7.97 (2H, d, J = 8 Hz, H-2', H-6'); 6.95 (2H, d, J = 8 Hz, H-3', H-5'), 6.42 (1 H, d, J = 2.5 Hz, H-6); δ 6.85 (1 H, d, J = 2.5 Hz, H-8); 6.88 (1 H, singlet, H-3); apiofuranoside moiety: δ 4.13 (m, H-5) & 4.02 (m, H-5'), 5.40 (1H, broad singlet, half line width, $\Delta\nu_{1/2}$ = 4 Hz, anomeric proton H-1); *E-p*-coumaroyl moiety: δ 6.20 (d, J = 16 Hz, H-8), 6.8 (d, J = 8 Hz, H-3 and H-5), 7.55 (d, J = 16 Hz, H-7), 7.6 (d, J = 8 Hz, H-2 and H-6). ¹³C NMR data of compound 2, (Table 1).

Table 1

¹³C NMR assignments of compounds (1) and (2) in DMSO-*d*₆.

Carbon	1	2	Free β -apiofuranose ^a
2	164.4	164.7	
3	103.8	103.5	
4	182.5	182.5	
5	161.5	161.5	
6	98.3	98.6	
7	162.7	162.0	
8	95.0	95.3	
9	157.0	157.4	
10	105.6	105.8	
1'	121.3	121.8	
2'	128.9	129.7	
3'	116.1	116.3	
4'	161.5	162.0	
5'	116.1	116.3	
6'	128.9	129.1	
β -apiofuranoside			
1''	109.3	109.0	103.4
2''	76.5	77.2	78.9
3''	79.8	79.9	80.5
4''	74.2	74.0	74.6
5''	64.10	65.0	65.3

¹³C assignments of 5''-mono-*E-p*-coumaroyl moieties in compound 2: (C-1) 125.0, (C-2) 130.7, (C-3) 115.5, (C-4) 162.9, (C-5) 115.5, (C-6) 130.7, (C-7) 145.1, (C-8) 115. (C-9) 166.43.

^a Data (Tenji Konishi et al., 1996).

2.5. In-vitro studies

2.5.1. DPPH assay

The estimation was done according to the method of Brand-Williams et al. (1995). All experiments were carried out in triplicate. Ascorbic acid was used as positive control.

2.5.2. Oxygen radical absorbance capacity (ORAC assay)

The antioxidant capacity of CEE, compound 1 and 2 in phosphate-buffered saline (10 mM, pH 7.4) were assayed by measuring the time of fluorescein fluorescence decay (Sigma), produced by 2,2'-azobis (2-amidinopropane) dihydrochloride (AAPH) in comparison with the positive control trolox (Lucas-Abellán et al., 2008).

2.5.3. Cell culture

RAW 264.7 macrophages cell line, was grown in adhesion on Petri dishes and maintained at 37 °C as described by Picerno et al. (2005).

2.5.4. Cytotoxic activity (MTT assay)

Cell viability was estimated by the MTT reduction assay (Lopes et al., 2012). The results of cell viability correspond to the mean \pm S.D. of at least four independent experiments performed in triplicate and are expressed as the percentage of the untreated control cells.

2.5.5. Analysis of NO (as total nitrites)

RAW 264.7 macrophages cells were harvested, plated to a seeding density of 1.5×10^6 in P60 well plates. After 2 h of cell adhesion, CEE (0.0625–1 mg/mL) or karafsin (0.0625–1 mg/mL) in PBS solution was added to the culture medium 1 h before and simultaneously to LPS (6×10^3 U mL⁻¹/24 h). Nitrite accumulation as NO release indicator, was measured in the culture medium by the Griess reaction (Green et al., 1982) 24 h after LPS challenge, according to Picerno et al. (2005). Amount of nitrite in each sample was calculated using a standard curve of freshly prepared sodium nitrite in culture medium and exposed to the positive control for NO production (LPS).

2.5.6. Assays of COX-2 and 5-LOX activities

RAW 264.7 macrophages were incubated for 72 h. After 24 h activation of culture is done by adding 1 μ L lipopolysaccharide then incubation for 24 h. CEE or karafsin were added after incubation for 24 h to a final concentration of 25, 50, 100, 500 mg/mL and incubated for 24 h. Diclofenac Sodium (100 mg/mL) was added and incubated for 24 h, used as standard and anti-inflammatory assay was done in pellet suspended in a small amount of supernatant. Measurement of the supernatant was done at 632 and 234 nm for COX-2 and 5-LOX activities, respectively (Viji and Helen, 2008).

2.6. Preparation of CEE topical gel formula

2.6.1. Preparation of CEE gel base

The gelling base sodium alginate was solubilized slowly while stirring in 80 mL of demineralized water for 30 min. Disodium edetate, triethanolamine and glycerin were dissolved in 20 mL water and stirred for 20 min with 2.5 g of CEE then added slowly to sodium alginate solution while stirring until a homogenous gel obtained (Mohamed, 2004).

2.6.2. Evaluation of the prepared CEE gel formula

2.6.2.1. Homogeneity. The prepared CEE topical gel was checked for homogeneity, gel appearance and absence of aggregates by visual inspection (Mohamed, 2004).

2.6.2.2. Extrudability study. Aluminum collapsible tube was filled with 10 g of celery gel and hold between fingers then tube was compressed by applying finger pressure and the extrudability percentage was

calculated (Mohamed, 2004; Ambala and Vemula, 2015).

2.6.2.3. pH value determination. By using digital pH meter pH value of gel was determined. Twenty-five mg of gel was dissolved in 100 mL of distilled water and the pH test was done. The pH of gel must be ideally near to normal pH of the skin (5.5) to avoid any irritation (Mohamed, 2004).

2.6.2.4. Celery topical gel formula content. One gm of celery topical gel was taken and solubilized in 50 mL phosphate buffer pH 5.5. The flask was kept for 1 h with shaken properly. The solution was filtered and 10 mL filtrate was taken and diluted and measured spectrophotometrically at 280 nm against phosphate buffer as blank. Celery extract content value gives a test for the dose uniformly of the gel formula (Ambala and Vemula, 2015).

2.6.2.5. Viscosity study. Brookfield viscometer was used to measure the viscosity of the prepared celery gel (Aiyalu et al., 2016).

2.6.2.6. Spreadability study. The Spreadability of celery topical gel was determined by calculating the spreading diameter of gel between two horizontal plates of 30 cm × 30 cm. The diameter of spreaded circle formed was determined (Aiyalu et al., 2016).

2.6.2.7. Grittiness. Under light microscope the celery gel tested for the presence of particles. Obviously, the gel preparation fulfils the requirement of freedom from particular matter and from grittiness is considered as ideal topical preparation (Aiyalu et al., 2016).

2.6.2.8. In-vitro diffusion study. The *in-vitro* diffusion study of prepared celery topical gel was carried out in diffusion cell apparatus according to Aiyalu et al. (2016). The cumulative amount of celery extract released was calculated and expressed in % plotted against time.

2.7. Determination of plant safety / acute toxicity

Median lethal dose (LD₅₀) of CEE was determined on groups each 6 male albino mice (30–35 g) after administration of single doses orally ranging from 1 to 2 g/kg b.wt. which represent the maximum soluble dose (Andress, 1992). No toxicity or mortality signs after oral administration of celery extract were observed in any group during 24 h. Thus, CEE was considered safe up to 2 g/kg b.wt. It is valued that the therapeutic doses would be 1/10 and 1/20 of the maximum soluble dose. Accordingly, doses that might be used in the *in-vivo* studies were (200 and 100 mg/kg) for CEE.

2.8. In- vivo anti-inflammatory activity of CEE topical gel formula

2.8.1. Experimental animals

The experiment was conducted using Albino Wistar rats of both genders weighing 160–200 g. The rats were kept in plastic cages in a controlled environment (25 °C ± 2 °C) and had unrestricted access to food and water. The procedure was conducted upon the approval of the ethics committee at October University for Modern Sciences and Arts (MSA) and according to the guidelines for the treatment and care of laboratory animals issued by the US National institute of Health (NIH publication 85–23 revised 1985).

2.8.2. Rat paw edema

The carrageenan model for induction of paw edema was employed to assess the anti-inflammatory activity of 1% CEE topical gel preparation against the topical standard marketed non-steroidal anti-inflammatory drug 1% diclofenac sodium. One percent of freshly prepared carrageenan (0.1 mL) was injected in the rats' right hind paw to induce inflammation and edema (Gupta and Kaur, 2015). A total of 18 rats were

randomly allocated into 3 groups (6 rats in each group). The untreated control group, where carrageenan was injected to induce inflammation and paw edema and no treatment was applied, the CEE topical gel group, where inflammation was induced and then celery topical gel was applied, and finally the diclofenac sodium group, where inflammation was induced and the standard diclofenac was applied. Both standard and test gel were applied to the sub-plantar tissue of the right hind paw of animal in 1 g quantity and gently rubbed using the index finger for 50 times after the carrageenan injection. The size (thickness) of the right hind paw was measured with a digital caliper before (0 h) and after the injection of the carrageenan at several time intervals (1, 2, 3 and 4 h) (Misal et al., 2012).

2.8.3. Percentage edema inhibition

Edema inhibition percentage was calculated as follows:

$$\text{Percentage inhibition} = 1 - (y - x / b - a) * 100$$

Where, x = test group initial paw thickness before treatment, y = test group paw thickness animal after treatment, a = control group initial paw thickness, b = control group final paw thickness.

2.8.4. Histopathological examination

The rat paw skin specimens were fixed in 10 % formol saline, trimmed off and then washed and dehydrated using ascending grades of alcohol. The dehydrated skin specimens were then washed using xylene, embedded in paraffin blocks and cut into 4–6 μm thick sections. Xylol was then utilized to remove the paraffin from the tissue sections and hematoxylin and eosin (H & E) were used for staining in order to perform the histological examination using the electric light microscope (Bancroft and Stevens, 2013). The stained sections were scored by two investigators in a blind fashion, and the degree of inflammation was assessed according to Hussein et al. (2013) and given a score from 0 to 5. The scores were defined as follows: 0 = no inflammation, 1 = mild inflammation, 2 = mild/moderate inflammation, 3 = moderate inflammation, 4 = moderate/severe inflammation and 5 = severe inflammation.

2.9. Statistical analysis

Data regarding MTT assay was expressed as % viability of RAW 264.7 macrophages. Statistical analysis was performed using Kaleida Graph 4.0 Synergy Software Inc (Reading, PA, USA). One-way ANOVA, followed by a Scheffemultiple range test, was used to determine the statistical significance in comparison to treated and untreated cells. NO production was expressed as percentages of inhibition calculated vs cell treated with LPS alone. All data were calculated from mean ± S.D. values of six independent experiments in triplicate. Statistical analysis was performed by ANOVA and multiple comparisons by Bonferroni test (Picerno et al., 2005). The p-value < 0.05 was statistically significant. The IC₅₀ value (dose giving 50 % inhibition of NO production) was calculated by graphic interpolation of the concentration–effect curves.

3. Results

3.1. Total phenolic and flavonoid contents

The total phenolic content in CEE was estimated as 189.17 ± 1.66 mg GAE/g. In addition, the total flavonoid content in the CEE was measured as 65.39 ± 0.35 mg CE/g. Thus, CEE was found to be a rich source of polyphenolic phytochemicals (Aryal et al., 2019).

3.2. Identification of polyphenols from CEE

Eight phenolics 1–8 from CEE, including two hitherto unknown natural products, namely, apigenin 7-O-mono-β-apiofuranoside 1 and 7-O-β-(5''-E-p-coumaroyl)-apiofuranoside, karafsin 2 together with the known phenolics; p-coumaric 3 (El Mousallami et al., 2002), caffeic acid

4 (Hussein et al., 2003), ferulic acid 5 (Hussein, 1997), *p*-hydroxy benzoic acid 6 (Hussein, 1997), chlorogenic acid 7 (Farah et al., 2008) and the flavone apigenin 8 (El Ansari et al., 1995). All structures were confirmed by direct interpretation of their spectral data, using high resolution mass spectrometry (HRESIMS), 1D- and 2D-NMR (HSQC, and HMBC).

3.2.1. Identification of apigenin-7-*O*- β -D-apiofuranoside 1

The negative HR-ESI-MS of compound 1 showed a pseudomolecular ion peak at m/z $[M-H]^-$ 401.4319 in accordance with a molecular formula of $C_{20}H_{17}O_9$ (calcd. 401.4333) indicating a molecular weight of 402 da (Dalton) for compound 1. ESI-MS-MS experiment showed further fragment at m/z 270 $[M-H-132]^-$, suggesting the presence of a pentosyl moiety ($C_5H_7O_4$) and at m/z 152 and m/z 118 ascribable to the Retro-Diels–Alder fragments of ring A and B of a flavone skeleton. The 1H NMR spectrum of 1 showed two doublets at δ 7.97 (2H, $J = 8$ Hz) and δ 6.95 (2H, $J = 8$ Hz), due to the equivalent 2',6' and 3',5', protons respectively, in ring B- of 4-oxygenated flavonoid. In addition, two meta coupled doublets, $J = 2.5$ Hz at δ 6.42 and δ 6.85 assignable to the H-6 and H-8 protons of ring A in 5,7-dihydroxy flavone and a singlet at δ 6.88 ascribable to H-3 proton of the C ring in that suggested flavone, respectively were also recognized. The ^{13}C NMR spectrum displayed 20 carbons (Table 1), whereas the HSQC spectrum gave a correlation between H-8 with the signal at δ 95.0 (C-8) and H-6 with signal at δ 99.81. The HMBC spectrum gave correlations between H-8 and C-6, C-7 and C-10. These set of experimental data led to identification of apigenin as the aglycone of compound 1 (El-Ansari et al., 1995). The β -apiofuranose moiety was confirmed by the presence of an anomeric proton at δ 5.40 (1H, broad singlet, half line width, $\Delta\nu_{1/2} = 4$ Hz), as well as from four other signals between δ 4.30 and δ 3.20 interfered by water protons and apigenin phenolic proton signals in the 1H NMR spectrum.

The recorded ^{13}C NMR spectrum of 1 exhibited two distinct pattern of carbon resonances typical for 7-*O* glycosylated apigenin and for apiofuranoside moieties (Table 1). The configuration of the β -apiofuranosyl moiety was assigned after hydrolysis of 1 with 2N aqueous HCl. The released aglycone was extracted from the hydrolysate by ethyl acetate and proved by CoPC (comparative paper chromatography) and UV spectral analysis to be apigenin. The aqueous acidic hydrolysate, thus left was freed from acid by being shaken twice with N, N-dimethyl octyl amine in $CHCl_3$. The left acid free aqueous solution was then dried under reduced pressure, at 50 °C and taken in some few drops of methanol. CoPC of the received dried hydrolysis product against authentic sugar markers. Using solvents (3) and (4) proved the identity of the hydrolysis sugar product to be β -apiose. The apiofuranosyl ring configuration was also confirmed by comparing 1H δ values with those reported for β -D-apiofuranose (Konishi et al., 1996). Furthermore, the recognized down field shift of δ value of the anomeric carbon in the recorded spectrum of 1 at δ 109.0, on comparison with the corresponding δ reported for the anomeric carbon of free apiofuranose and the subsequent up field shift of δ value of the apiofuranose C-2 moiety to δ 76.5 ppm in the ^{13}C NMR spectrum of 1, in comparison with δ 78.9 ppm for C-2 in free apiofuranose is obviously due to substitution at the anomeric carbon of 1 by the apigenin moiety. Similar shifts were reported by (Markham et al., 1978). The HMBC spectrum confirmed the location of the apiose at C-7 of apigenin by showing connectivity between the anomeric hydrogen of apiose and the carbon at δ 162.7 (C-7). The HSQC spectrum furnished all the direct correlations between protons and corresponding carbons. Comparison with literature data also confirmed the ^{13}C values for apigenin -7-*O*-glycoside (El-Ansari et al., 1995). Thus, the structure of 1 could be deduced as being the new flavone glycoside, apigenin-7-*O*-mono- β -D-apiofuranoside (Fig. 1).

3.2.2. Identification of apigenin-7-*O*- β -(5''-*E*-*p*-coumaroyl)-apiofuranoside, karafsin 2

A light brown amorphous powder, showed chromatographic properties (dark purple spot on paper chromatogram under UV light, turning

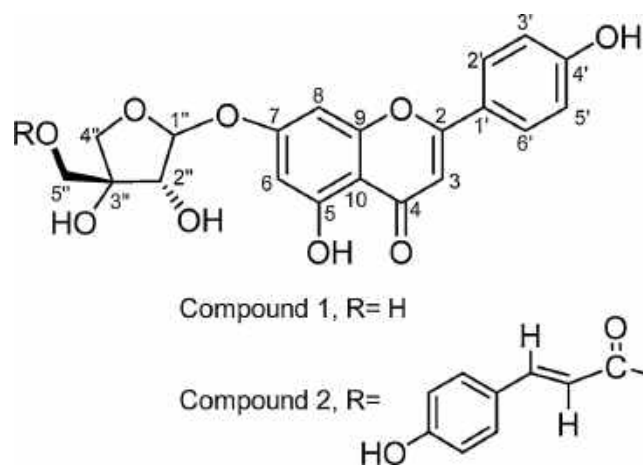


Fig. 1. Chemical structures of apigenin-7-*O*- β -D-apiofuranoside (1) and apigenin-7-*O*- β -(5''-*E*-*p*-coumaroyl)-apiofuranoside, karafsin (2).

lemon yellow when fumed with ammonia vapor, moderate migration in aqueous and organic solvents, reminiscent of flavone glycosides. UV spectral analysis in methanol and on addition of shift reagents (Mabry et al., 1970) confirmed the presence of a free hydroxyl at 4'-position (stable MeONa spectrum) and a substituted hydroxyl at the 7-position (no shift with NaOAc) of that proposed flavone structure. Normal acid hydrolysis of 2 (2N aqueous HCl, 2 h, 100 °C) yielded apiose (comparative paper chromatography, Co-PC), apigenin and *p*-coumaric acid (Co-PC, UV spectral and 1H NMR). Consequently, 2 is apigenin-7-*O*- β -(*E*-*p*-coumaroyl) -apioside. The HRESIMS (negative-ion mode) of compound 2 exhibited a pseudomolecular ion peak at $[M-H]^-$ 547.4889 corresponding to a molecular weight 548 D, ascribable to a molecular formula of $C_{29}H_{23}O_{11}$ (calcd 547.4876) Further fragment ion peaks were observed in the ESI-MS-MS spectrum at m/z 401 $[M-H-146]^-$ and m/z 269 $[M-H-146-132]^-$ corresponding to the successive loss of *p*-coumaroyl and pentosyl moieties. In order to determine unambiguously the structure of 2, especially the site of attachment of the *p*-coumaroyl moiety it was necessary to apply NMR spectroscopic analysis. The 1H -NMR spectrum of 2 (DMSO- d_6 , room temperature) revealed two distinct methylene proton resonances at δ ppm 4.13 & 4.02 (each *m*) assignable to a C-5 methylene apioside carbon attached at the C-7 apigenin carbon (HMQC and HMBC). Resonances of the C-2 and C-4 apioside protons appeared more upfield in the region from δ 3.3–3.9, overlapped with water protons signal. In this spectrum an anomeric proton, assigned to the C-1 apiofuranosyl unit, was found resonating at δ 5.20 (*d*, $J = 3$ Hz). The characteristic protons of the *E*-*p*-coumaroyl moiety resonated in this spectrum at δ 6.20 (*d*, $J = 16$ Hz, H-8), 6.8 (*d*, $J = 8$ Hz, H-3 and H-5), 7.55 (*d*, $J = 16$ Hz, H-7), 7.6 (*d*, $J = 8$ Hz, H-2 and H-6). The spectrum showed in addition, the presence of a 7-*O* substituted apigenin moiety by the proton resonances at δ 6.40 (*d*, $J = 2.5$ Hz) and 6.80 (*d*, $J = 2.5$ Hz), assignable to the H-6 and H-8 of this moiety. These two chemical shift values were closely similar to those reported for the corresponding proton resonances in the spectrum 7-*O*-apioside apigenin 1. In this spectrum the chemical shifts of the B ring proton resonances (See experimental) were found to be in close agreement with the proposed structure. The ^{13}C NMR analysis of 2 confirmed proposed structure. As expected, the spectrum (DMSO- d_6 , room temperature) exhibited five distinct apioside carbon resonances (Table 1). The anomeric carbon resonance was recognized from the downfield signal at δ 109.0, while the most upfield resonances at δ 64.94 was assigned to the methylene C-5 apioside carbon bearing the *p*-coumaroyl moiety. The ^{13}C NMR shifts of the aglycone part of 2, (Table 1) corresponded well with the shifts for apigenin, with the only significant difference being those corresponding to C-6, C-7 and C-8. These shifts are analogous to those reported when the 7- hydroxy group, in a flavone is glycosylated

(Agrawal, 1989). From the assigned aglycon and sugar carbon signals values, deduced from HSQC experiments it was apparent that a *p*-coumaroyl mono saccharide unit was attached to C-7 of the aglycone. The chemical shifts of all the individual protons of the sugar unit were attributed on the basis of the ^{13}C chemical shifts of their relative attached carbons which were clearly assigned from the HSQC spectrum. These data showed the presence of β -*p*-coumaroyl-apiofuranosyl moiety substituted at its C-5 apiose carbon as indicated by the downfield shift of this C-5 signal (46.94) signal. An unambiguous determination of the linkage site was followed from the HMBC spectrum, which showed key ^3J correlation cross peaks between the anomeric proton of the apiose at δ 5.3 and the C-7 of the apigenin at 162.00; and between the C-5 apiose protons (δ 4.13 and 4.02) and the carbonyl carbon of the *p*-coumaroyl moiety (δ 166.43). The β -configuration at the anomeric position for the apiofuranosyl unit followed from its coupling constant. Therefore, the structure of **2** was determined as the new flavone glycoside, Apigenin-7-*O*- β -(5''-*E*-*p*-coumaroyl)- β -apiofuranoside, for which we suggest the name Karafsin (Fig. 1).

3.3. In-vitro studies

3.3.1. DPPH assay

The antioxidant capacity of the CEE, apigenin-7-*O*- β -apiofuranoside **1** and karafsin were determined using the DPPH assay. The EC_{50} values were $5.5 \pm 1.02 \mu\text{g/mL}$, $3.5 \pm 2.13 \mu\text{g/mL}$ and $1.5 \pm 2.13 \mu\text{g/mL}$ respectively compared with the positive control Vit. C (EC_{50} of $1.83 \pm 1.41 \mu\text{g/mL}$) which indicates powerful antioxidant capacity of apigenin 7-*O*-mono-apiofuranoside and karafsin.

3.4. ORAC assay

The antioxidant capacity of CEE, apigenin 7-*O*-mono-apiofuranoside and karafsin were determined using the ORAC assay. The EC_{50} values were $4.2 \pm 1.42 \mu\text{g/mL}$, $2.85 \pm 1.99 \mu\text{g/mL}$ and $1.85 \pm 1.99 \mu\text{g/mL}$ respectively which were much lower than the positive control Trolox, which had an EC_{50} of $28.0 \pm 14.3 \mu\text{g/mL}$, further confirming the high antioxidant activity of apigenin 7-*O*-mono-apiofuranoside and karafsin.

3.5. Assessment of cytotoxic activity (MTT assay)

Before the evaluation of the potential *in vitro* anti-inflammatory activity of CEE, the potential cytotoxicity of CEE and karafsin towards RAW 264.7 macrophages cell line was evaluated by (MTT) reduction assay. RAW264.7 cells were exposed to CEE and karafsin for 24 h. At h 24 only ethanol extract and karafsin showed a significant difference for

concentrations equal or greater than 0.5 mg/mL. The results indicated that celery extract treatment of raw macrophages highly induced the cell proliferation, starting from the treated concentration (0.5 mg/mL), which led to $5.56 \pm 2.52 \%$ of control increase in the cell proliferation ($P < 0.05$). On the other hand, karafsin treatment with raw macrophages highly induced the cell proliferation significantly ($P < 0.001$), starting from the concentration 0.5 mg/mL, which led to $15.16 \pm 2.43 \%$ of control increase in the cell proliferation as shown in (Fig. 2). The highest concentration tested (1 mg/mL) increased cell viability by $10.22 \pm 2.42 \%$ of control ($P < 0.001$). At the same concentration (1 mg/mL), karafsin increases cell viability by $20.61 \pm 2.51 \%$ of control ($P < 0.001$) as shown in (Fig. 2).

3.5.1. Assessment of COX-2 activity

The effects of CEE and karafsin on production of prostaglandins were evaluated by *in-vitro* COX-inhibitor screening assay of COX-2 activity. The percentage inhibition at different concentrations was calculated and the results are presented in (Fig. 3 a). Both CEE and karafsin inhibited COX-2 activity in a dose-dependent manner; there was an increase in the inhibitory activity of both with a rise in the concentration. The results exhibit that CEE and karafsin have affinity toward COX-2. The extract and karafsin at 100 and 500 mg/mL displayed significant COX-2 inhibitory activity with the extent of inhibition in the range of $65.76 \pm 2.67 \%$, $73.39 \pm 3.1 \%$, $70.33 \pm 2.97 \%$ and $79.35 \pm 2.68 \%$, respectively. Diclofenac sodium was used as positive control.

3.5.2. Assessment of 5-LOX activity

LOX inhibition is potential for the treatment of allergy, inflammatory disorders and cancer. Due to this reason, the effects of CEE and karafsin on leukotrienes production were determined by the inhibition of 5-LOX activity and the results are shown in (Fig. 3b). Inhibition of LOX by the non-steroidal anti-inflammatory drugs is in the same manner to that of rat mast cell LOX, and can be used as an indicative screen for such activity (Katsori et al., 2011). Both CEE and karafsin inhibited 5-LOX activity in a dose-dependent manner; there was an increase in the inhibitory activity of both with a rise in the concentration. The initial screening showed that CEE and karafsin at 100 and 500 mg/mL were strong inhibitors of 5-LOX with the extent of inhibition in the range of $70.39 \pm 2.86 \%$, $75.12 \pm 2.67 \%$, $75.77 \pm 2.57 \%$ and $83.21 \pm 2.88 \%$, respectively. Diclofenac sodium was used as positive control.

3.5.3. Analysis of nitric oxide (NO)

During inflammation NO production is increased by the inducible nitric oxide synthase (iNOS) which is an important inflammatory mediator. The *in-vitro* activity of CEE and karafsin on NO production by

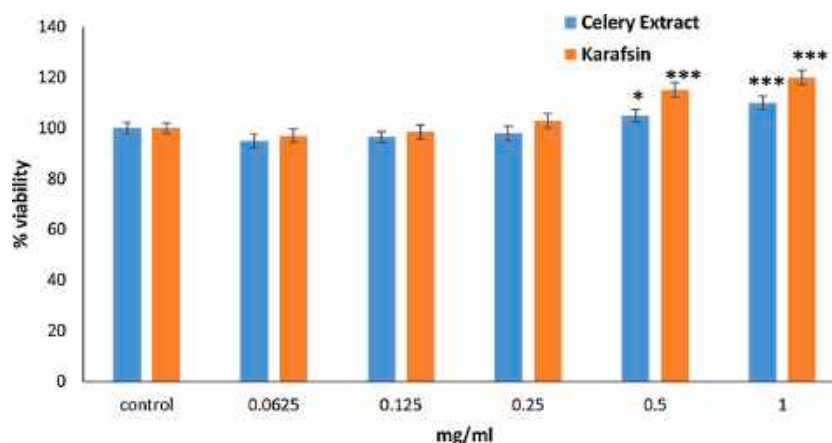


Fig. 2. Viability of RAW 264.7 macrophages treated with CEE and karafsin for 24 h; The data represent the percentage of macrophage viability at each concentration (mean \pm S.D.), $n = 4$.

Statistical significance using One-way ANOVA, followed by a Scheffemultiple range test: * $p < 0.05$, ** $p < 0.01$, *** $p < 0.001$.

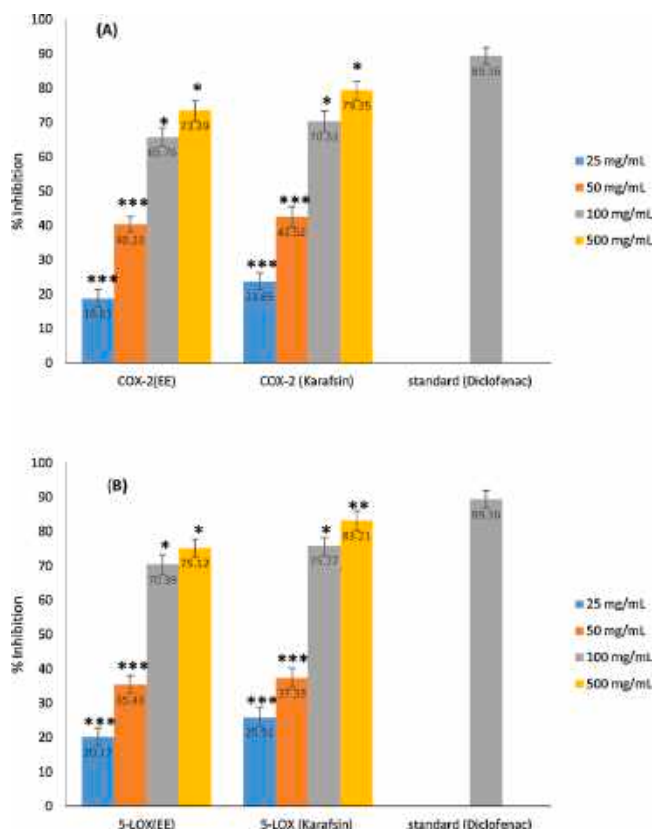


Fig. 3. (A) Effect of CEE and karafsin on inhibition of prostaglandins using the cyclooxygenase-2 (COX-2) inhibitory assays, (B) Effect of celery ethanol extract and karafsin on inhibition of leukotrienes using the 5-lipoxygenase (5-LOX) inhibitory assay. Inhibition obtained (%) is expressed as mean ± S.D. of the mean of three independent experiments performed in triplicate. One-way Anova followed by Tukey-Posthoc -Test were used to determine the statistical significance: * p < 0.05, ** p < 0.01, *** p < 0.001.

LPS-stimulated RAW264.7 macrophages were assessed. Percentage of NO was calculated against control (Aquino et al., 2002) which is shown in (Fig. 4). Cells were pre-incubated for 2 h with both CEE and karafsin and then exposed for 22 h to LPS as shown in (Fig. 4), at non-toxic concentrations CEE decreased NO levels in a dose-dependent manner (IC₅₀ = 0.254 mg/mL). At the highest concentration tested (1 mg/mL), it decreased NO levels by 62.95 ± 3.94 %. On the other hand, karafsin was able to decrease NO levels in a dose-dependent manner

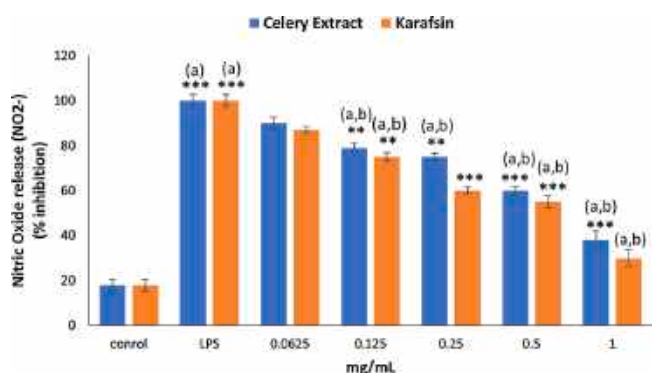


Fig. 4. Effect of CEE and karafsin on NO production by LPS-stimulated RAW 264.7 macrophages; Results are presented as mean ± S.D. of the mean of six independent experiments performed in triplicate. (a) significant difference from control (b) significant difference from LPS. Statistical significance using One-way ANOVA, followed by by Bonferroni test: * p < 0.05, ** p.

Table 2

Evaluation of celery ethanol extract topical gel formula.

Test	Result
Appearance	Yellowish white color
Homogeneity	homogenous
Extrudability study	Good (80 %)
pH	5.5 ± 0.68
Drug content	98.1 % and 98.96 %
Viscosity	2500 ± 0.32 cp
Spreadability	3.67 ± 0.23
Grittiness	Absent

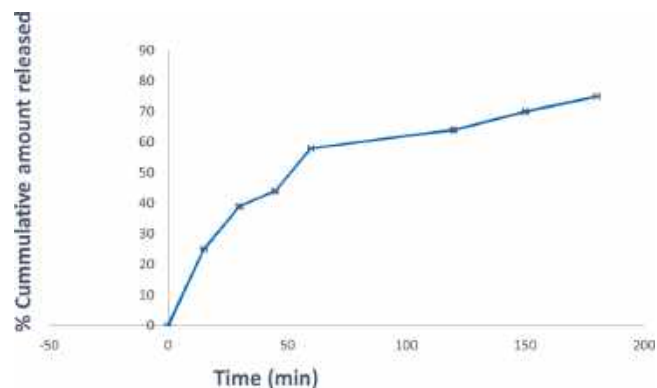


Fig. 5. *In-vitro* diffusion study of CEE gel formulation. % Cumulative amount celery extract released is expressed as mean ± S.D. of the mean of three independent experiments performed in triplicate.

(IC₅₀ = 0.177 mg/mL). At the highest tested concentration (1 mg/mL), it decreased NO levels by 71.25 ± 3.65 % (Fig. 4).

3.6. Evaluation CEE topical gel formula

The developed gel was tested for color, clarity and homogeneity by visual inspection after the gel has been set in the container. It was tested for appearance, pH value, gel content, and rheological properties. Sodium alginate gel showed transparent appearance with excellent smooth homogeneity and free of any aggregates with suitable spreadability and extrudability values (Table 2). pH shows excellent value of 5.5 ± 0.68 which was suitable for skin applications and the extract content of gel was found 98.5 %. The consistency reflects the capacity of the gel, to get ejected in uniform and desired quantity when the tube was squeezed. Consistency is inversely proportional to the distance travelled by falling cone. The consistency of the substance is one of the most important features to anti-inflammatory topical formulations due to being applied to the thin layers of the skin. The gel was of excellent viscosity value to be spread well on the skin. *In-vitro* diffusion study through cellophane

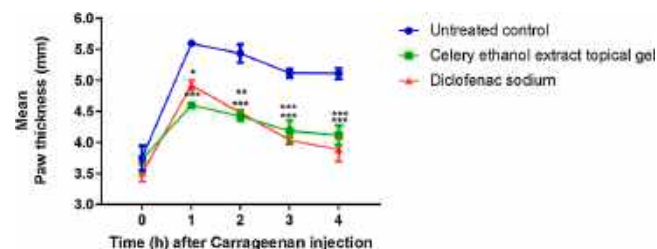


Fig. 6. Effect of topical application of CEE gel. Data were analyzed using One-way ANOVA followed by Tukey's Test. Each value represents the mean ± S.D. for n=6. Values are compared to the untreated control group, * p < 0.05, **p < 0.01, ***p < 0.001.

membrane has shown 75 % cumulative celery extract released after 3 h and it was increasing with time (Fig. 5). Hence the gel preparation fulfils the entire requirements as desired for any topical formulation.

3.7. In-vivo studies

3.7.1. Evaluation of anti-inflammatory activity of CEE topical gel formula

The effect of CEE topical gel formula on carrageenan-induced paw edema in rats were shown in (Fig. 6). The injection of carrageenan generated an inflammatory reaction and edema leading to an increase in the rat paw size. Celery gel was able to significantly ($p < 0.001$) inhibit

rat paw edema in a time dependent manner compared with the untreated control group, with a maximum percentage inhibition of 79.51 % observed after 4 h of carrageenan injection using diclofenac sodium gel 1% as a standard gel formulation.

3.7.2. Histopathological examination

Normal group: Control animals showed normal histological structure of rat paw skin. The skin of paw is characterized by a thick epidermal layer covered with a deeply eosinophilic keratin layer. The dermal layer is composed of dense fibrous connective tissue and few number of blood capillaries without any inflammatory reaction score

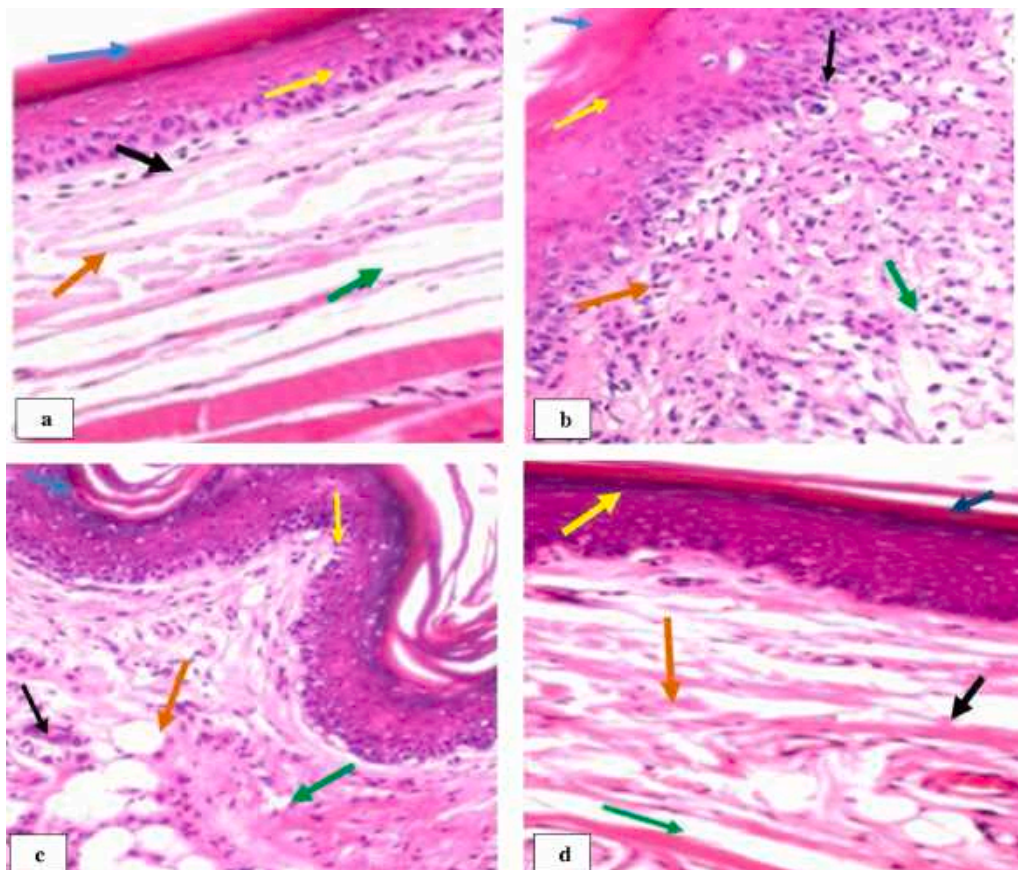


Fig. 7. Histopathologic examination representative photographs from the skin showing the protective effect of the celery topical gel formulation against carrageenan-induced inflammation in rats. Control group (a) Control rats showed normal histological structure of paw skin of rat showing average skin epidermis with average keratin (blue arrow), average dermis with average pilo-sebaceous units (black arrow), average hair follicles (red arrow) and average superficial (yellow arrow) and deep blood vessels (green arrow), untreated control group (b), Inflammation induced in paw skin treated with carrageenan, showing epidermis with detached keratin (blue arrow), markedly edematous dermis with few hair follicles (black arrow), mildly dilated superficial (red arrow) and markedly dilated deep blood vessels (green arrow), marked inflammatory infiltrate extending to underlying bone (yellow arrows), celery gel formulation (c), rats treated by celery extract as anti-inflammatory drug showing mild epidermal edema (blue arrow), dilated superficial blood vessels (black arrow), and marked edema with mild inflammatory infiltrate extending to underlying muscles (red arrows), standard group (d), rats treated by diclofenac as an anti-inflammatory drug showing average epidermis with average keratin (blue arrow), dermis with few small-sized hair follicles (black arrow), mildly dilated superficial (red arrow) and deep blood vessels (green arrow), and mild edema extending to subcutis (yellow arrow). (e) Semi-quantitative assessment of pathological changes induced by carrageenan. **a** Normal group: Tissue section of rat paw skin showing normal histological structure score 0 (H&E x400). **b** Injured group: Tissue section of rat paw skin showing massive inflammatory cells infiltration arrow score 4 (H&E x400). **c** - Test Group: Tissue section of rat paw skin treated by celery ethanol extract topical gel formulation showing low grade of inflammatory cells infiltration arrow score 2 (H&E x400). **d**: Standard group: Tissue section of rat paw skin treated by diclofenac sodium showing marked reduction of inflammatory reaction score 1(H&E x400).

0 (Fig. 7a). **Untreated control Group:** Carrageenan-induced inflammation in paw skin characterized by cellular infiltration, mainly polymorphonuclear leucocytes (PMNL), eosinophils, lymphocytes and macrophages at the borderline between the dermis and subcutis. Congestion and edema of dermal blood capillaries and edema were also observed score 4 (Fig. 7b). **Test Group:** CEE topical gel was able to reduce inflammation, where there was a significant decrease in inflammatory cell infiltration compared with the injured group. Also, the dermal layer revealed mild edema with less prominent dilatation of the blood vessels score 2 (Fig. 7c). **Standard Group:** Diclofenac treated group showed mild inflammatory cells infiltration compared with the injured group. Also, mild congestion of blood capillaries and low intensity of edema were seen in the dermal layer score 1 (Fig. 7d).

4. Discussion

Plant polyphenols and flavonoids have been previously reported to have both *in-vitro* and *in-vivo* anti-inflammatory activity. In addition, recent studies illustrated that specific flavonoids, especially flavone derivatives from the class of the new isolates, show *in-vitro* anti-inflammatory activity by modulating pro-inflammatory gene expression. They include iNOS, COX-2 and other several pivotal cytokines (Sharma et al., 2007; Lim et al., 2019). The process of inflammation also incorporates the activation of inflammatory mediators like neutrophil derived free radicals and reactive oxygen species (ROS) (Conforti et al., 2008; Udegbunam et al., 2012). Large number of derivatives of the acylated flavonoids (the class of karafsin) can be found in different plants and also in human diet. They are reported to have different biological activities such as anti-oxidant, anticancer and antimicrobial activity (Mohammed et al., 2015; Amen et al., 2015; Salem et al., 2011).

Despite the reported anti-inflammatory activity of other varieties of celery, there is no data in the literature on *Apium graveolens* var. *secalinum* Alef leaf phytoconstituents, anti-inflammatory activity and, its mechanism of action.

The results of this study showed that CEE with its high content of polyphenols and the new acylated flavonoid karafsin may all of them responsible for the biological activity of celery. The ability of CEE and karafsin to neutralize free radicals during the inflammation, and the suppression of NO, 5-LOX and COX-2 in RAW 264.7 macrophages cells (without significantly affecting cell viability which was > 90 % at all tested concentrations) might contribute to the inhibitory impact on progression of inflammatory reaction mediators thanks to the presence of the acylated flavonoids (Udegbunam et al., 2012).

Moreover, CEE was found safe at an oral LD50 > 2 gm/kg in rats. CEE topical gel formulation 1% was able to significantly reduce rat paw edema by 79.51 % after 4 h of treatment as well as infiltration of inflammatory cells compared with the untreated group. The observed results were comparable to that of the standard group of diclofenac sodium gel 1%.

Phytochemical investigation of CEE resulted in the isolation of unique acylated flavonoid, 7-O- β -(5''-E-p-coumaroyl)-apiofuranside, karafsin, and the hitherto unknown, apigenin 7-O-mono- β -apiofuranside, together with 6 known polyphenols. Polyphenols 1–8 isolated from CEE reported to have antioxidant and/or anti-inflammatory activity. Apigenin and its derivatives reported to inhibit both COX-2 and iNOS in a dose-dependent manner with reduction of macrophage M-CSF-induced proliferation without affecting cellular viability (Comalada et al., 2006). *Oldenlandia diffusa* may exert its anti-inflammatory effects *via p*-coumaric acid, in a mechanism that included the suppression of inflammatory cell infiltration, as well as the levels of TNF- α and IL-6 (Zhu et al., 2018). Caffeic acid mediates multiple cell protection mechanisms, involving both anti-inflammatory and anti-oxidant effects by decreasing NF- κ B and IL-1 β expression in the cochlea and opposing the oxidative/nitrosative damage induced by noise insult (Paciello et al., 2020). Nile et al. (2016) reported that the results presented for ferulic acid, caffeic acid and *p*-coumaric revealed excellent anti-inflammatory

activities evaluated by TNF- α and IL-6 inhibition assays compared to dexamethasone. *Para*-hydroxybenzoic acid is reported to be capable of mitigating oxidative stress induced by hydrogen peroxide, which is thought to contribute to neuronal cell death in neurodegeneration and potent neuroprotective under conditions of excitotoxicity. Meanwhile it showed no anti-inflammatory activity in microglial cells stimulated with lipopolysaccharide (Winter et al., 2017). In addition, chlorogenic acid significantly inhibited not only NO production but also the expression of COX-2 and iNOS, without any cytotoxicity. Chlorogenic acid also attenuated pro-inflammatory cytokines (including IL-1 β and TNF- α) and other inflammation-related markers such as IL-6 in a dose-dependent manner. (Hwang et al., 2014). This supports the current results suggesting synergistic activity of CEE polyphenols. Therefore, CEE possesses potential as a potent natural anti-inflammatory candidate.

5. Conclusion

CEE showed high polyphenols and flavonoids content, in addition significant *in vitro* antioxidant activity for CEE and karafsin. Our results clearly indicated the *in-vitro* inhibitory activity of CEE and karafsin on NO release, COX-2 and 5-LOX, when added before LPS stimulation in the medium of J774.A1 cells. The 1% CEE topical gel was able to significantly reduce rat paw edema and inflammation. The results are comparable to those observed in the standard diclofenac sodium group, with almost the same potency. The anti-inflammatory and anti-edematous properties exhibited by CEE might be due to reduction of NO production and inhibition of both COX-2 and 5-LOX and also can be attributed, at least partly, to its content of acylated flavonoid derivatives. This is evidenced by their anti-oxidant properties and ability to inhibit COX-2, 5-LOX and NO release. It is concluded that CEE should be used in both pharmaceutical and food industries in different conditions of inflammation.

Funding

This research received no external funding.

CRediT authorship contribution statement

Eman S. Mostafa: Conceptualization, Methodology, Formal analysis, Validation, Investigation, Writing - original draft, Writing - review & editing. **Mahmoud A.M. Nawwar:** Supervision. **Dalia A. Mostafa:** Methodology. **Mai F. Ragab:** Methodology. **Noha Swilam:** Conceptualization, Methodology, Formal analysis, Validation, Investigation, Writing - original draft, Writing - review & editing.

Declaration of Competing Interest

The authors declare no conflict of interest.

References

- Abdou, A.M., Abdallah, H.M., Mohamed, M.A., Fawzy, G.A., Abdel-Naim, A.B., 2013. A new anti-inflammatory triterpene saponin isolated from *Anabasis setifera*. Arch. Pharm. Res. 36, 715–722. <https://doi.org/10.1007/s12272-013-0075-9>.
- Agrawal, P.K., 1989. Carbon-13 NMR of Flavonoids. Studies in Organic Chemistry. Amsterdam, New York. p.xvi, 564.
- Aiyalu, R., Govindarajan, A., Ramasamy, A., 2016. Formulation and evaluation of topical herbal gel for the treatment of arthritis in animal model. Braz. J. Pharm. Sci. 52, 493–507. <https://doi.org/10.1590/s1984-82502016000300015>.
- Akanda, M.R., Uddin, M.N., Kim, I.S., Ahn, D., Tae, H.J., Park, B.Y., 2019. The biological and pharmacological roles of polyphenol flavonoid tilianin. Eur. J. Pharmacol. 842, 291–297. <https://doi.org/10.1016/j.ejphar.2018.10.044>.
- Al-Saeed, A., 2011. Gastrointestinal and cardiovascular risk of nonsteroidal anti-inflammatory drugs. Oman Med. J. 26, 385–391. http://www.omjournal.org/full_text_PDF.aspx?DetailsID=163&type=fulltext.
- Ambala, R., Vemula, S.K., 2015. Formulation and characterization of ketoprofen emulgels. Int. J. Appl. Pharm. Sci. Res. 5, 112–117. <https://doi.org/10.7324/JAPS.2015.50717>. <https://www.japsonline.com/admin/php/uploads/1562.pdf.pdf>.

- Amen, Y.M., Marzouk, A.M., Zaghoul, M.G., Afifi, M.S., 2015. A new acylated flavonoid tetraglycoside with anti-inflammatory activity from *Tipuana tipu* leaves. *Nat. Prod. Res.* 29, 511–517. <https://doi.org/10.1080/14786419.2014.952233>.
- Andress, J.M., 1992. In: Chengelis, C.P. (Ed.), *The Mouse: Toxicology, Acute Toxicity Studies. Animal Models in Toxicology* Gad SC. Marcel Dekker, New York.
- Aquino, R., Morelli, S., Tomaino, A., Pellegrino, M., Saija, A., Grumetto, L., Puglia, C., Ventura, D., Bonina, F., 2002. Antioxidant and photoprotective activity of a crude extract of *Culcitium reflexum* H.B.K. leaves and their major flavonoids. *J. Ethnopharmacol.* 79, 183–191. [https://doi.org/10.1016/S0378-8741\(01\)00379-8](https://doi.org/10.1016/S0378-8741(01)00379-8).
- Aryal, S., Baniya, M.K., Danekhu, K., Kunwar, P., Gurung, R., Koirala, N., 2019. Total phenolic content, flavonoid content and antioxidant potential of wild vegetables from western Nepal. *Plants Basel (Basel)* 8 (4), 96. <https://doi.org/10.3390/plants8040096>.
- Bancroft, J.D., Stevens, A., 2013. *Theory and Practice of Histological Techniques*. Churchill Livingstone, Edinburgh; New York.
- Brand-Williams, W., Cuvelier, M.E., Berset, C.L.W.T., 1995. Use of a free radical method to evaluate antioxidant activity. *LWT - J Food Sci Technol.* 28, 25–30. [https://doi.org/10.1016/S0023-6438\(95\)80008-5](https://doi.org/10.1016/S0023-6438(95)80008-5).
- Comalada, M., Ballester, I., Bailón, E., 2006. Inhibition of pro-inflammatory markers in primary bone marrow-derived mouse macrophages by naturally occurring flavonoids: analysis of the structure-activity relationship. *Biochem. Pharmacol.* 72 (8), 1010–1021. <https://doi.org/10.1016/j.bcp.2006.07.016>.
- Conforti, F., Sosa, S., Marrelli, M., Menichini, F., Statti, G.A., Uzunov, D., Tubaro, A., Menichini, F., Della Loggia, R., 2008. In vivo anti-inflammatory and in vitro antioxidant activities of Mediterranean dietary plants. *J. Ethnopharmacol.* 116, 144–151. <https://doi.org/10.1016/j.jep.2007.11.015>.
- El Mousallami, A.M., Afifi, M.S., Hussein, S.A., 2002. Acylated flavonol diglucosides from *Lotus polyphyllus*. *Int. J. Pharmacol. Phytochem. Ethnomedicine* 60, 807–811. [https://doi.org/10.1016/S0031-9422\(02\)00177-2](https://doi.org/10.1016/S0031-9422(02)00177-2).
- El-Ansari, M.A., Nawwar, M.A., Saleh, N.A., 1995. Stachysetin, a diapienin-7-glucoside-p, p'-dihydroxy-truxinate from *Nachys aegyptiaca*. *Int. J. Pharmacol. Phytochem. Ethnomedicine* 40, 1543–1548. [https://doi.org/10.1016/0031-9422\(95\)00395-N](https://doi.org/10.1016/0031-9422(95)00395-N).
- Farah, A., Monteiro, M., Donangelo, C.M., Lafay, S., 2008. Chlorogenic acids from green coffee extract are highly bioavailable in humans. *J. Nutr.* 138, 2309–2315. <https://doi.org/10.3945/jn.108.095554>.
- Green, L.C., Wagner, D.A., Glogowski, J., Skipper, P.L., Wishnok, J.S., Tannenbaum, S.R., 1982. Analysis of nitrate, nitrite, and [15N]nitrate in biological fluids. *J. Anal. Biochem.* 126, 131–138. [https://doi.org/10.1016/0003-2697\(82\)90118-X](https://doi.org/10.1016/0003-2697(82)90118-X).
- Gupta, R., Kaur, J., 2015. Evaluation of analgesic, antipyretic and anti-inflammatory activity on *Cordia dichotoma* G. Forst. Leaf. *J. Pharmacognosy Res.* 7, 126–130. <https://doi.org/10.4103/0974-8490.147227>.
- Hörl, W.H., 2010. Nonsteroidal anti-inflammatory drugs and the kidney. *J. Pharm (Basel)*. 3, 2291–2321. <https://doi.org/10.3390/ph3072291>.
- Hussain, T., Tan, B., Yin, Y., Blachier, F., Tossou, M.C., Rahu, N., 2016. Oxidative stress and inflammation: What polyphenols can do for us? *J. Oxid Med Cell Longev.* <https://doi.org/10.1155/2016/7432797>.
- Hussein, S.A., 1997. New dimeric phenolic conjugates from the wood of *Tamarix tetragyna*. *J. Nat. Prod. Sci.* 3, 127–134. <http://www.scopus.com/inward/record.url?eid>.
- Hussein, S.A., Ayoub, N.A., Nawwar, M.A., 2003. Caffeoyl sugar esters and an ellagitannin from *Rubus sanctus*. *Int. J. Pharmacol. Phytochem. Ethnomedicine* 63, 905–911. [https://doi.org/10.1016/S0031-9422\(03\)00331-5](https://doi.org/10.1016/S0031-9422(03)00331-5).
- Hussein, S.Z., Yusoff, K.M., Makpol, S., Yusof, Y.A.M., 2013. Gelam honey attenuates carrageenan-induced rat paw inflammation via NF- κ B pathway. *J. PLoS One.* 8, e72365. <https://doi.org/10.1371/journal.pone.0072365>.
- Hwang, S.J., Kim, Y.W., Park, Y., Lee, H.J., Kim, K.W., 2014. Anti-inflammatory effects of chlorogenic acid in lipopolysaccharide-stimulated RAW 264.7 cells. *Inflamm. Res.* 63 (1), 81–90. <https://doi.org/10.1007/s00011-013-0674-4>.
- Katsori, A.M., Chatzopoulou, M., Dimas, K., Kontogiorgis, C., Patsilinos, A., Trangas, T., Hadjipavlou-Litina, D., 2011. Curcumin analogues as possible anti-proliferative & anti-inflammatory agents. *Eur. J. Med. Chem.* 46, 2722–2735. <https://doi.org/10.1016/j.ejmech.2011.03.060>.
- Konishi, T., Inoue, T., Kiyosawa, S., Fujiwara, Y., 1996. A 2,5-dimethoxytetrahydrofuran from *Hemerocallis fulva* var. *kwanso*. *Phytochemistry* 42 (1), 135–137. [https://doi.org/10.1016/0031-9422\(96\)83285-7](https://doi.org/10.1016/0031-9422(96)83285-7).
- Kooti, W., Daraei, N., 2017. A review of the antioxidant activity of celery (*Apium graveolens* L.). *J. Evid-Based Complatt. Altern. Med.* 22, 1029–1034. <https://doi.org/10.1177%2F2156587217717415>.
- Langhansova, L., Landa, P., Kutil, Z., Tauchen, J., Marsik, P., Rezek, J., Lou, J.D., Yun, Z., Vanek, T., 2017. Myrica rubra leaves as a potential source of a dual 5-LOX/COX inhibitor. *Food Agric. Immunol.* 28, 343–353. <https://doi.org/10.1080/09540105.2016.1272554>.
- Larkcom, J., 2008. *Oriental Vegetables: the Complete Guide for the Gardening Cook*, 2nd ed. Kodansha International, New York.
- Liemburg-Apers, D.C., Willems, P.H.G.M., Koopman, W.J.H., 2015. Interactions between mitochondrial reactive oxygen species and cellular glucose metabolism. *Arch. Toxicol.* 89, 1209–1226. <https://doi.org/10.1007/s00204-015-1520-y>.
- Lim, H., Heo, M.Y., Kim, H.P., 2019. Flavonoids: broad spectrum agents on chronic inflammation. *Biomolther* 27 (3), 241–253. <https://doi.org/10.4062/biomolther.2019.034>.
- Lopes, G., Sousa, C., Silva, L.R., Pinto, E., Andrade, P.B., Bernardo, J., Mouga, T., Valentão, P., 2012. Can phlorotannins purified extracts constitute a novel pharmacological alternative for microbial infections with associated inflammatory conditions. *J. PLoS One.* 7, e31145. <https://doi.org/10.1371/journal.pone.0031145>.
- Lucas-Abellán, C., Mercader-Ros, M.T., Zafrilla, M.P., Fortea, M.I., Gabaldón, J.A., Núñez-Delgado, E., 2008. ORAC-fluorescein assay to determine the oxygen radical absorbance capacity of resveratrol complexed in cyclodextrins. *J. Agric. Food Chem.* 56, 2254–2259. <https://doi.org/10.1021/jf0731088>.
- Mabry, T.J., Markham, K.R., Thomas, M.B., 1970. *The Systematic Identification of Flavonoids*. Springer-Verlag, New York.
- Malhotra, S.Ke., 2006. *Handbook of Herbs and Spices*. J. Woodhead publishing.
- Markham, K.R., Ternai, B., Stanley, R., Geiger, H., Mabry, T.J., 1978. Carbon-13 NMR studies of flavonoids—III: Naturally occurring flavonoid glycosides and their acylated derivatives. *J. Tetrahedron.* 3, 1389–1397. [https://doi.org/10.1016/0040-4020\(78\)88336-7](https://doi.org/10.1016/0040-4020(78)88336-7).
- Misal, G., Dixi, T.G., Gulkari, V., 2012. Formulation and evaluation of herbal gel. *Indian J. Nat. Prod. Resour.* 3 (4), 501–505. <http://nopr.niscair.res.in/handle/123456789/15563>.
- Mohamed, M.I., 2004. Optimization of chlorphenesin emulgel formulation. *AAPS J.* 6, 81–87. <https://doi.org/10.1208/aapsj060326>.
- Mohammed, R.S., El Souda, S.S., Taie, H.A., Moharam, M.E., Shaker, K.H., 2015. Antioxidant, antimicrobial activities of flavonoids glycoside from *Leucaena leucocephala* leaves. *Int. J. Appl. Pharm. Sci. Res.* 5, 138–147. <https://japsonline.com/admin/php/uploads/1544.pdf>.
- Moro, C., Palacios, L., Lozano, M., D'Arrigo, M., Guillamón, E., Villares, A., Martínez, J. A., García-Lafuente, A., 2012. Anti-inflammatory activity of methanolic extracts from edible mushrooms in LPS activated RAW 264.7 macrophages. *Food Chem.* 130 (2), 350–355. <https://doi.org/10.1016/j.foodchem.2011.07.04>.
- Nile, S.H., Ko, E.Y., Kim, D.H., Keum, Y.S., 2016. Screening of ferulic acid related compounds as inhibitors of xanthine oxidase and cyclooxygenase-2 with anti-inflammatory activity. *Rev. Bras. Farmacogn.* 26 (1), 50–55. <https://doi.org/10.1016/j.bjpr.2015.08.013>.
- Paciello, F., Antonella Di Pino, A., Rolesi, R., Troiani, D., Paludetti, G., Grassi, C., Feroni, A., 2020. Anti-oxidant and anti-inflammatory effects of caffeic acid: in vivo evidences in a model of noise-induced hearing loss. *Food Chem. Toxicol.* <https://doi.org/10.1016/j.fct.2020.111555>. In press.
- Picerno, P., Autore, G., Marzocco, S., Meloni, M., Sanogo, R., Aquino, R.P., 2005. Anti-inflammatory activity of verminoside from *Kigelia africana* and evaluation of cutaneous irritation in cell cultures and reconstituted human epidermis. *J. Nat. Prod.* 68, 1610–1614. <https://doi.org/10.1021/np058046z>.
- Poyton, R.O., Ball, K.A., Castello, P.R., 2009. Mitochondrial generation of free radicals and hypoxic signaling. *Trends Endocrinol. Metab.* 20, 332–340. <https://doi.org/10.1016/j.tem.2009.04.001>.
- Ramana, K.V., Srivastava, S., Singhal, S.S., 2014. Lipid peroxidation products in human health and disease 2014. *J. Oxid Med Cell Longev* 2014, 1–3. <https://doi.org/10.1155/2014/162414>.
- Rubatzky, V.E., Yamaguchi, M., 1997. *World Vegetables: Principles, Production, and Nutritive Values* S, 2nd ed. Chapman & Hall, New York.
- Salem, J.H., Chevalot, I., Harscoat-Schiavo, C., Paris, C., Fick, M., Humeau, C., 2011. Biological activities of flavonoids from *Nitraria retusa* (Forssk.) Asch. and their acylated derivatives. *Food Chem.* 124, 486–494. <https://doi.org/10.1016/j.foodchem.2010.06.059>.
- Sharma, J.N., Al-Omran, A., Parvathy, S.S., 2007. Role of nitric oxide in inflammatory diseases. *Inflammopharmacol* 15, 252–259. <https://doi.org/10.1007/s10787-007-0013-x>.
- Udegbunam, R.I., Nwamkpa, O.K., Udegbunam, S.O., Nwaehujor, C.O., Offor, G.E., 2012. Evaluation of anti-inflammatory activities of root extracts of *Stephania dinklagei* (Engl.)Diels. *Afr. J. Pharm. Pharmacol.* 6 (11), 834–839.
- Viji, V., Helen, A., 2008. Inhibition of lipoxygenases and cyclooxygenase-2 enzymes by extracts isolated from *Bacopa monniera* (L.) Wettst. *J. Ethnopharmacol.* 118, 305–311. <https://doi.org/10.1016/j.jep.2008.04.017>.
- Winter, A.N., Brenner, M.C., Punessen, N., Snodgrass, M., Byars, C., Arora, Y., Linseman, D.A., 2017. Comparison of the Neuroprotective and anti-inflammatory effects of the anthocyanin Metabolites, protocatechuic acid and 4-hydroxybenzoic Acid. *Oxid. Med. Cell. Longev.* 2017, 1–13. <https://doi.org/10.1155/2017/6297080>.
- Zhang, X., Xiao, W., Hu, X., 2018. Predicting essential proteins by integrating orthology, gene expressions, and PPI networks. *J. PLoS One.* 13 (4), e0195410. <https://doi.org/10.1371/journal.pone.0195410>.
- Zhu, H., Liang, Q., Xiong, X., Wang, Y., Zhang, Z., Sun, M., Lu, X., Wu, D., 2018. Anti-inflammatory effects of p-coumaric acid, a natural compound of *Oldenlandia diffusa*, on arthritis model rats. *Evid. Complement. Alternat. Med.* 2018, 1–9. <https://doi.org/10.1155/2018/5198594>.
- Zilic, S., Serpen, A., Akilloğlu, G., Gökmen, V., Vančetović, J., 2012. Phenolic compounds, carotenoids, anthocyanins, and antioxidant capacity of colored maize (*Zea mays* L.) kernels. *J. Agric. Food Chem.* 60, 1224–1231. <https://doi.org/10.1021/jf204367z>.